Reactive collision between alkali-metal atoms and halogen molecules

Babaji Charan Mishra
Department of Physics, Buxi Jagabandhu Bidyadhar College, Bhubaneswar 751014, India

Trilochan Pradhan
Utkal University, Bhubaneswar 751004, India
and Institute of Physics, Bhubaneswar 751005, India
(Received 5 February 1991)

The Feynman diagram method for atomic collisions developed by us has been applied to reactive collisions between alkali-metal atoms and halogen molecules. The velocity-averaged differential and total cross sections for the production of alkali halide molecules have been calculated and compared with available experimental results.

PACS number(s): 34.50.Lf, 82.30.Hk, 82.40.Dm

I. INTRODUCTION

The large cross section of the formation of alkali halide molecules observed in the reactive collision between an alkali-metal atom and a halogen molecule has been of great interest for the past 50 years. In order to explain the large cross sections measured through flame studies [1–3] and cross-beam techniques [4,5], the "harpoon-reaction" model was first proposed by Polanyi [1] and later on developed by Magee [6]. According to this model, when the two reactants (alkali-metal atom M and halogen molecule X_2) approach each other, the alkali-metal atom releases its valence electron like a harpoon to the halogen molecule (the target), which results in the formation of a negatively charged halogen molecular ion X_2^- whose dissociation energy is smaller than that of the halogen molecule X_2. The lowering of dissociation energy of X_2 by the electron attachment results in the dissociation of the X_2^- into X and X^-. The Coulomb force acts as the rope that pulls the halide ion (X^-) toward the alkali-metal ion (M^+). The sequence of processes can be represented as

$$M+X_2 \rightarrow M^+ + X_2^- \rightarrow M^+X^- + X \rightarrow MX + X \ . \quad (1)$$

The necessary condition for such a reaction is that the electron affinity of the halogen molecule should be high and the ionization potential of the alkali-metal atom be low. This condition is connected with the fact that the rapid transfer of an electron from the alkali-metal atom M to the halogen molecule X_2 occurs in the region of the crossing between the covalent M-X_2 and the ionic M^+-X_2^- potential-energy curves. The internuclear distance r_c at which the electron jumps from M to X_2 is obtained from the principle of conservation of energy, i.e.,

$$\frac{e^2}{r_c} = \varepsilon_M - \varepsilon_a \ , \quad (2)$$

where ε_M is the ionization potential of the alkali-metal atom and ε_a is the electron affinity of the halogen molecule. As it is assumed that the electron transfer occurs at the crossing distance r_c with unit probability, the total reaction cross section is given as

$$\sigma_M = \pi r_c^2 = \frac{\pi e^4}{(\varepsilon_M - \varepsilon_a)^2} \ . \quad (3)$$

As r_c for most of the reactions calculated from Eq. (2) is of the order of 10 Å, one has an explanation for the abnormally high cross section. It may be pointed out that Magee's formula for the total cross section given in Eq. (3) does not take into consideration the dissociation of the halogen molecule X_2. If this is taken into account, one gets

$$\frac{e^2}{r_c} = \varepsilon_M + D_{X_2} - \varepsilon_a \quad (4)$$

in place of (2) and the cross section gets modified to

$$\sigma = \frac{\pi e^4}{(\varepsilon_M + D_{X_2} - \varepsilon_a)^2} \ , \quad (5)$$

D_{X_2} being the dissociation energy of X_2.

Although extremely simple in nature, this model describes the basic mechanism of the chemical dynamics involved [7–9]. During the past few years, some attempts have, however, been made to take into account the transition probability from the covalent to the ionic states [10], the angular momentum of collision, and the interaction between covalent and ionic states [11,12]. These are essentially refinements of the harpoon model.

Apart from having abnormally large cross sections, the harpoon reactions are characterized by two other features: much of the alkali halide molecules recoil forward with respect to the incident beam of alkali-metal atoms and most of the chemical energy released appears as a vibrational excitation of the alkali halide molecule. These characteristics, therefore, suggest that a stripping mechanism [4,7,13], which is used in nuclear reaction theory (Butler theory), holds good for harpoon reactions. But the harpoon model does not tell anything about angular distribution.

In a series of experiments, by photochemical methods, Davidovits and collaborators [14,15] have measured the cross sections of the product of alkali halide molecules in the reactive collisions of alkali-metal atoms and halogen molecules and have concluded that the harpoon model did not provide an adequate quantitative description for the reaction. Further, a large number of experiments have been done by various workers [16–20], which show that the center-of-mass angular distributions of the reactive cross sections are mostly peaked along the forward direction. It seems that there does not exist any satisfactory theoretical explanation for such distributions.

In our quantum-field-theoretic approach to atomic collisions [21,22], we have shown that electron-transfer processes in atomic collisions can be calculated very simply by the Feynman diagrammatic method. Not only is the method simple from a calculational point of view, it also provides a graphic model to visualize all possible channels of atomic collision processes. We propose to apply this method to the problem of reactive collision between alkali-metal atoms and halogen molecules.

We organize the paper in the following manner. In Sec. II, we briefly outline the Hamiltonian approach within the framework of quantum-field theory for the interaction among nonrelativistic bound systems involving two particles and their constituents and justify its applicability to the collisions involving molecules. In Sec. III, we present the Feynman diagram that gives the dominant contribution for the harpoon reaction leading to the formation of an alkali halide molecule in the reactive collision between an alkali-metal atom and a halogen molecule, calculate both differential and total cross sections, and compare the results with those of experiment and other theories. Finally, in Sec. IV, we discuss the relative merit of our calculations.

II. NONRELATIVISTIC FIELD THEORY FOR COLLISIONS BETWEEN BOUND SYSTEMS

The problem that one would encounter in perturbation theory for the scattering of particles that can form bound states is that such states would not come out of the theory unless they were used as inputs. For instance, in nonrelativistic electron-proton collision, it would be necessary to put the hydrogen atom, in addition to the electron and the proton, into the Hamiltonian before carrying out perturbation calculations for scattering processes. In order to do this, one would have to represent the proton, the electron, and the hydrogen atom by second-quantized field operators $p(\mathbf{x}_1,t)$, $e(\mathbf{x}_2,t)$, and $h(\mathbf{x}_1,\mathbf{x}_2,t)$, respectively. By separating the center of mass and relative coordinates, the interaction Hamiltonian can be written in terms of a hydrogen-proton-electron vertex,

$$\Gamma_n(b\mathbf{k}-a\mathbf{q})=\int d^3x\, e^{i(b\mathbf{k}-a\mathbf{q})\cdot\mathbf{x}} v(x) u_n(\mathbf{x}) , \tag{6}$$

where $u_n(\mathbf{x})$ is the c-number energy eigenfunction of hydrogen, $v(x)$ is the potential that leads to the formation of the bound system and $\mathbf{k}$ and $\mathbf{q}$ are the momenta of the proton and the electron, respectively, with $a=M/(M+m)$, $b=m/(M+m)$, M and m being the masses of the proton and the electron, respectively. It is interesting to note that the vertex function is the Fourier transform of the product of the potential and the wave function of the bound state. In order to obtain the matrix element for the process we require the propagators for the center-of-mass motion of the hydrogen atom $G_n(\mathbf{P},P_0)$, that of the proton $\Delta_p(\mathbf{k},k_0)$ and that of the electron $\Delta_e(\mathbf{q},q_0)$, which can be written as

$$G_n(\mathbf{P},P_0)=\left[P_0-\frac{P^2}{2(M+m)}+\varepsilon_n+i\eta\right]^{-1} , \tag{7a}$$

$$\Delta_p(\mathbf{k},k_0)=\left[k_0-\frac{k^2}{2M}+i\eta\right]^{-1} , \tag{7b}$$

$$\Delta_e(\mathbf{q},q_0)=\left[q_0-\frac{q^2}{2m}+i\eta\right]^{-1} . \tag{7c}$$

The details of the calculations of the matrix elements are given in our paper [22]. The simple vertex function described here can be generalized to the case of a composite and its fragments and used in the Feynman-diagram approach to complex atomic and molecular collisions.

III. HARPOON REACTION

A. Matrix element

As mentioned above, the harpoon reaction is a two-step mechanism in which there is an electron transfer followed by an atom transfer as represented in Eq. (1). The lowest-order dominant Feynman diagram for the general harpoon reaction between an alkali-metal atom (M) and a halogen molecule (X_2), producing an alkali halide molecule (MX) and a halogen atom (X) can be represented by Fig. 1. In principle, higher-order diagrams can be drawn, but these would involve more vertices and propagators of ions, atoms, and molecules, on account of which their contributions would be very small compared to the lowest-order diagram considered above. The energies of the ions, atoms, and molecules represented by the lines are easily seen to be

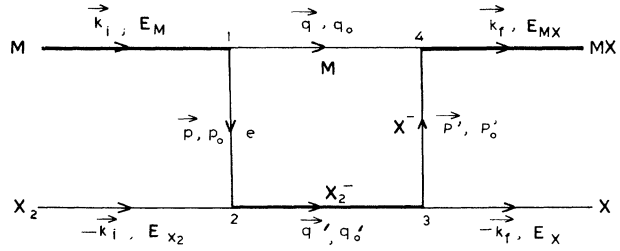

FIG. 1. Feynman diagram for the harpoon reaction $M+X_2\rightarrow MX+X$.

$$E_M=\frac{k_i^2}{2m_M}-\varepsilon_M,\quad E_{X_2}=\frac{k_i^2}{4m_X}-D_{X_2},$$
$$E_{MX}=\frac{k_f^2}{2(m_M+m_X)}-\varepsilon_{MX},\quad E_X=\frac{k_f^2}{2m_X},$$
$$E_q=\frac{q^2}{2m_M},\quad E_{q'}=\frac{q'^2}{4m_X}-\varepsilon_a,$$
$$E_p=\frac{p^2}{2m_e},\quad E_{p'}=\frac{p'^2}{2m_X}, \tag{8}$$

where m_M is the mass of the alkali-metal atom, m_X is the mass of the halogen atom, m_e is the mass of the electron, ε_M is the ionization potential of the alkali-metal atom, D_{X_2} is the dissociation energy of the halogen molecule, ε_{MX} is the binding energy of M^+ and X^- in the MX molecule, and ε_a is the electron affinity of the halogen molecule. The matrix element for this diagram can be written with the help of the Feynman rules prescribed in our paper [22] as

$$M(\mathbf{k}_i,\mathbf{k}_f)=\frac{i}{(2\pi)^4}\int\int\int\int d^4q\,d^4q'd^4p\,d^4p'\delta^4(k_i-q-p)\delta^4(p-k_i-q')\delta^4(q'-p'+k_f)$$
$$\times\Gamma_1(\mathbf{p},\mathbf{q})\Gamma_2(\mathbf{p},\mathbf{q}')G_e(p)G_{X_2^-}(q')\Gamma_3(\mathbf{p}',\mathbf{k}_f)G_{X^-}(p')\Gamma_4(\mathbf{p}',\mathbf{q})G_{M^+}(q), \tag{9}$$

where the Γ's are the vertex functions and the G's are the propagators. Making use of the momentum dependence of the vertex function, that for $c\leftrightarrow a+b$ is given as

$$\Gamma(c\leftrightarrow a+b)=\Gamma\left[\frac{m_a\mathbf{k}_b-m_b\mathbf{k}_a}{m_c}\right]. \tag{10}$$

and that of a propagator has the form

$$G_\alpha(p)=\left[p_0-\frac{p^2}{2m_\alpha}+i\eta\right]^{-1}, \tag{11}$$

and neglecting the electron mass as compared to other masses, the above matrix element reduces to

$$M(\mathbf{k}_i,\mathbf{k}_f)=\frac{i}{(2\pi)^4}\int_{-\infty}^{+\infty}dq_0\int d^3q\frac{\Gamma_1(\mathbf{q}-\mathbf{k}_i)\Gamma_2(\mathbf{q}-\mathbf{k}_f)\Gamma_3(\mathbf{q}/2-\mathbf{k}_f)\Gamma_4(\mathbf{q}-\alpha\mathbf{k}_f)}{D_aD_bD_cD_d}, \tag{12}$$

where

$$D_a=q_0-\frac{q^2}{2m_M}+i\eta,$$
$$D_b=E_M-q_0-\frac{(\mathbf{k}_i-\mathbf{q})^2}{2m_e}+i\eta,$$
$$D_c=E_M-q_0+\varepsilon_a-D_{X_2}+\frac{k_i^2-q^2}{4m_X}+i\eta,$$
$$D_d=E_M-q_0+\frac{k_i^2}{4m_X}-\frac{k_f^2}{2m_X}-D_{X_2}-\frac{(\mathbf{k}_f-\mathbf{q})^2}{2m_X}+i\eta,$$

and

$$\alpha=\frac{m_M}{m_M+m_X}. \tag{13}$$

The q_0 integration can now be performed using Cauchy's theorem and Eq. (12) reduces to

$$M(\mathbf{k}_i,\mathbf{k}_f)=-\int\frac{d^3q}{(2\pi)^3}\frac{\Gamma_1(\mathbf{q}-\mathbf{k}_i)\Gamma_2(\mathbf{q}-\mathbf{k}_i)\Gamma_3(\mathbf{q}/2-\mathbf{k}_f)\Gamma_4(\mathbf{q}-\alpha\mathbf{k}_f)}{\left[\frac{(\mathbf{q}-\mathbf{k}_i)^2}{2\mu_M}+\varepsilon_M\right]\left[\frac{(\mathbf{q}-\alpha\mathbf{k}_f)^2}{2\mu_{MX}}+\varepsilon_{MX}\right]\left[\frac{k_i^2-q^2}{2\mu_i}-\varepsilon_M-D_{X_2}+\varepsilon_a\right]}, \tag{14}$$

where μ_M is the reduced mass of the alkali-metal atom; $\mu_{MX}=m_Mm_X/(m_M+m_X)$, the reduced mass of the alkali halide molecule; and $\mu_i=2m_Mm_X/(m_M+2m_X)$, the reduced mass of the (MX_2) system. The remaining integration can be performed after getting explicit forms for the vertex functions that require the knowledge of the respective wave functions and potentials. Without any loss of generality, the potential and the wave functions for the

(M^+e) and (M^+X^-) systems can be taken to be Coulombic, in which case

$$\Gamma_1(\mathbf{q}-\mathbf{k}_i)=\frac{4\pi^{1/2}e^2s_1^{3/2}}{(\mathbf{q}-\mathbf{k}_i)^2+s_1^2}\ ,$$
$$\Gamma_4(\mathbf{q}-\alpha\mathbf{k}_f)=\frac{4\pi^{1/2}e^2s_4^{3/2}}{(\mathbf{q}-\alpha\mathbf{k}_f)^2+s_4^2}\ , \tag{15}$$

where the s's are the inverse of the first Bohr radii and are given as

$$s_1^2=2\mu_M\varepsilon_M\approx 2m_e\varepsilon_M\ ,$$
$$s_4^2=2\mu_{MX}\varepsilon_{MX}\ . \tag{16}$$

Substituting (13) in (12), we get

$$M(\mathbf{k}_i,\mathbf{k}_f)=-\frac{1}{(2\pi)^3}\int d^3q\frac{g_1(\mathbf{q}-\mathbf{k}_i)\Gamma_2(\mathbf{q}-\mathbf{k}_i)\Gamma_3(\mathbf{q}/2-\mathbf{k}_f)g_4(\mathbf{q}-\alpha\mathbf{k}_f)}{(k_i^2-q^2)/2\mu_i-\varepsilon_M-D_{X_2}+\varepsilon_a}\ , \tag{17}$$

where

$$g_1(\mathbf{q}-\mathbf{k}_i)=\frac{8\pi^{1/2}s_1^{5/2}}{[(\mathbf{q}-\mathbf{k}_i)^2+s_1^2]^2}\ ,$$
$$g_4(\mathbf{q}-\alpha\mathbf{k}_f)=\frac{8\pi^{1/2}s_4^{5/2}}{[(\mathbf{q}-\alpha\mathbf{k}_f)^2+s_4^2]^2} \tag{18}$$

are Fourier transforms of the Coulombic bound wave functions of the (M^+e) and (M^+X^-) systems, respectively.

The determination of the matrix element demands the knowledge of the vertex function for X_2, e and X_2^- and that for X_2^-, X and X^-; and these, in turn, require the potential energy of the interaction between X_2 and e as well as X and X^-. These potentials determine the respective scattering matrices, which are represented by the Feynman diagrams of Figs. 2 and 3, respectively.

Keeping in mind the fact that the Fourier transforms of these matrix elements give the required potentials, we obtain for the diagrams of Fig. 2,

$$V_a(r)=\frac{e^2}{a_0'}\left[\frac{1}{D}-\left[\frac{1}{D}+\frac{1}{b'}\right]e^{-2D/b'}\right]\ , \tag{19a}$$

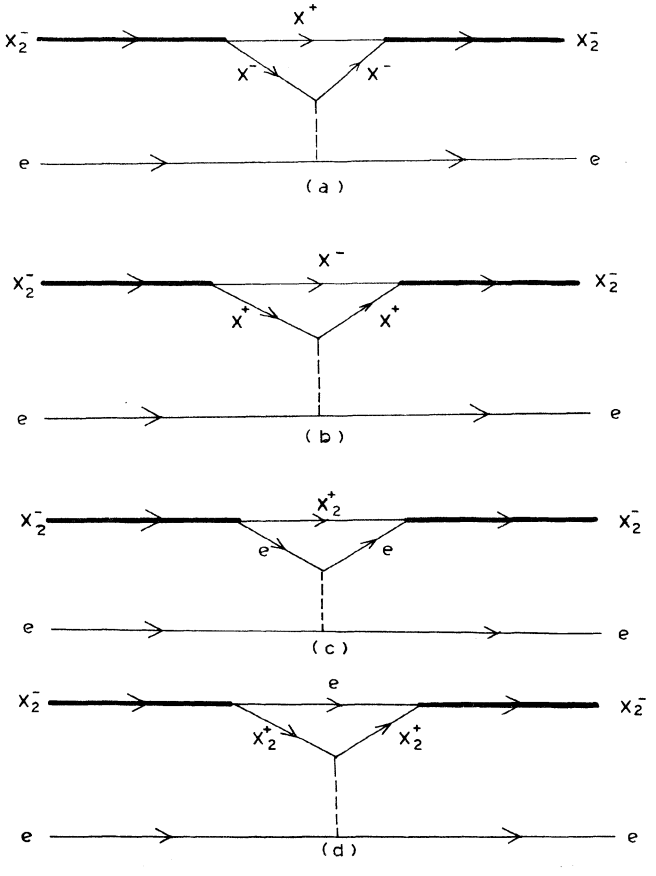

FIG. 2. Feynman diagrams for the vertex $X_2+e\rightarrow X_2^-$.

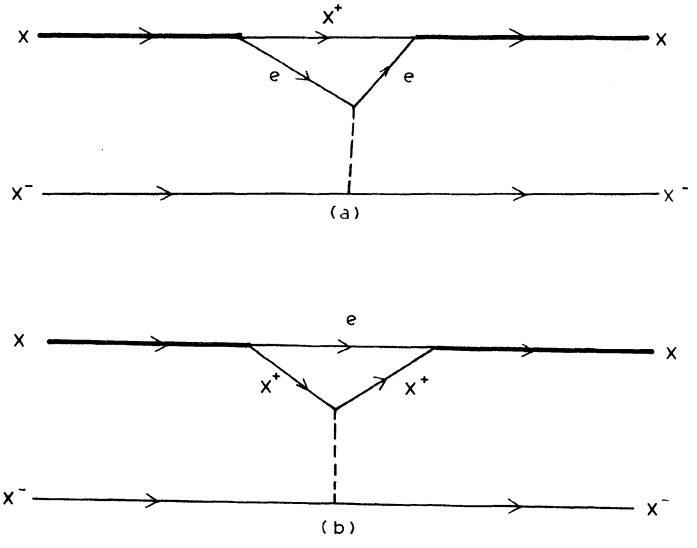

FIG. 3. Feynman diagrams for the vertex $X_2^-\rightarrow X+X^-$.

$$V_b(r)=-\frac{e^2}{a_0'}\left[\frac{1}{D}-\left[\frac{1}{D}+\frac{1}{a'}\right]e^{-2D/a'}\right], \tag{19b}$$

$$V_c(r)=\frac{e^2}{a_0}\left[\frac{1}{D}-\left[\frac{1}{D}+\frac{1}{b}\right]e^{-2D/b}\right], \tag{19c}$$

$$V_d(r)=-\frac{e^2}{a_0}\left[\frac{1}{D}-\left[\frac{1}{D}+\frac{1}{a}\right]e^{-2D/a}\right], \tag{19d}$$

where

$$a_0'=\frac{2}{m_X e^2},\quad D=r/a_0,\quad a'=1/2+\beta,\quad b'=1/2-\beta,$$

$$a_0=\frac{1}{m_e e^2},\quad a=\beta,\quad b=1-\beta,$$

and

$$\beta=\frac{m_e}{2m_X}.$$

Since β is infinitesimally small, we have in the limit

$$\beta\to 0,$$

$$V(r)=V_a(r)+V_b(r)+V_c(r)+V_d(r)$$

$$=-\frac{e^2}{a_0}\left[1+\frac{1}{D}\right]e^{-2D}, \tag{20}$$

which is the Hartree potential.

In order to obtain the potential between X and X^-, the Feynman diagrams in Fig. 3 are to be evaluated. The corresponding potentials work out to be

$$V_a(r)=\frac{e^2}{a_0}\left[\frac{1}{D}-\left[\frac{1}{D}+\frac{1}{b}\right]e^{-2D/b}\right],$$

$$V_b(r)=-\frac{e^2}{a_0}\left[\frac{1}{D}-\left[\frac{1}{D}+\frac{1}{a}\right]e^{-2D/a}\right], \tag{21}$$

with $a=2\beta$ and $b=1-2\beta$. The sum of the potentials due to both the diagrams in the limit $\beta\to 0$ turns out to be the same as in the previous case, which is the Hartree potential given in Eq. (20).

We shall take the neutral composite to be like a hydrogen atom and the charged one to be like an electron with proper mass factors so that the wave function for the vertex will be like that of an H^- ion. This wave function, as given by Tietz [23], is

$$\phi_0(r)=\frac{a_0}{2\sqrt{\pi}}\left[2k_0\left[k_0+\frac{2}{a_0}\right]\left[2k_0+\frac{2}{a_0}\right]\right]^{1/2}$$

$$\times\frac{e^{ik_0 r}}{2r}(1-e^{-2r/a_0}). \tag{22}$$

Making use of appropriate potentials and wave functions the required $X_2+e\to X_2^-$ vertex function works out to be

$$\Gamma(\mathbf{K})=-\frac{4\pi^{1/2}e^2[k_0(k_0+2s_0)(k_0+s_0)]^{1/2}}{K^2+(k_0+2s_0)^2}, \tag{23}$$

where $k_0=(2m_e\varepsilon_a)^{1/2}$, ε_a being the electron affinity of X_2 and $s_0=a_0^{-1}=(2m_e I_{X_2})^{1/2}$, and I_{X_2} being the ionization potential of X_2 breaking up into X_2^+ and e. The expression for the $X_2^-\to X+X^-$ vertex is obtained from the $X_2+e\to X_2^-$ vertex given above by replacing (i) k_0 by $k_0'=(m_X D_{X_2-})^{1/2}$, D_{X_2-} being energy of dissociation of X_2^- into X and X^- and (ii) s_0 by $s_0'=a_0'^{-1}=(2m_e I_X)^{1/2}$, I_X being the ionization potential of X to break up into X^+ and e.

On substitution of such functions for $\Gamma_2(\mathbf{q}-\mathbf{k}_i)$ and $\Gamma_3(\mathbf{q}/2-\mathbf{k}_f)$ in Eq. (17), it is found that $g_1(\mathbf{q}-\mathbf{k}_i)$ and $\Gamma_2(\mathbf{q}-\mathbf{k}_i)$ are sharply peaked at $\mathbf{q}=\mathbf{k}_i$. We can, therefore, evaluate the integral by taking the rest of the integrand with its value at $q=k_i$ outside the integral. We obtain

$$M(\mathbf{k}_i,\mathbf{k}_f)=\frac{128\pi e^4 s_1^{3/2}s_4^{5/2}[k_0(k_0+s_0)(k_0+2s_0)]^{1/2}}{(\varepsilon_M+D_{X_2}-\varepsilon_a)[s_1+(k_0+2s_0)]^2}$$

$$\times\frac{[k_0'(k_0'+s_0')(k_0'+2s_0')]^{1/2}}{[k_i^2/4+k_f^2-k_i k_f x+(k_0'+2s_0')^2][k_i^2+\alpha^2 k_f^2-2\alpha k_i k_f x+s_4^2]^2}, \tag{24}$$

where $x=\cos\theta=\hat{k}_i\cdot\hat{k}_f$, θ being the c.m. scattering angle.

B. Cross sections

The differential cross section, in terms of the matrix element, is written as

$$\frac{d\sigma}{d\Omega}=\frac{\mu_f^2}{4\pi}\frac{v_f}{v_i}\left|M(\mathbf{k}_i,\mathbf{k}_f)\right|^2, \tag{25}$$

where μ_f is the reduced mass of the (MX-X) system in the outgoing channel and v_i and v_f are the relative velocities in the incoming and outgoing channels, respectively. From the conservation of energy, we obtain

$$\frac{v_f}{v_i}=\left[2\alpha\left[1-\frac{\varepsilon_M+D_{X_2}-\varepsilon_{MX}}{E_i}\right]\right]^{1/2}, \tag{26}$$

where $E_i=k_i^2/2\mu_i$ is the relative energy in the incoming channel. If the masses are expressed in terms of atomic weights, the differential cross section works out to be

$$\frac{d\sigma}{d\Omega}=\frac{2^{13}(A_M+A_X)^3(2\alpha)^{1/2}}{A_M(A_M+2A_X)^2}\frac{k_f}{k_i}\frac{\varepsilon_M^{5/2}\varepsilon_{MX}^{5/2}D_{X_2}^{3/2}-\varepsilon_a^{3/2}}{(\varepsilon_M^{1/2}+\varepsilon_a^{1/2}+2I_{X_2}^{1/2})^4}\frac{(1+\sqrt{I_{X_2}/\varepsilon_a})(1+2\sqrt{I_{X_2}/\varepsilon_a})e^4}{(\varepsilon_m+D_{X_2}-\varepsilon_a)^2}\frac{1}{(A-Bx)^2(C-Bx)^4}, \tag{27}$$

where A_M is the atomic weight of an alkali-metal atom, A_X is the atomic weight of a halogen atom,

$$A=\frac{4A_ME_i}{A_M+2A_X}\left[\frac{k_f^2}{k_i^2}+\frac{1}{4}\right]+D_{X_2}-,\quad B=\frac{4A_ME_i}{A_M+2A_X}\frac{k_f}{k_i},\quad C=\frac{2\alpha A_ME_i}{A_M+2A_X}\left[\frac{k_f^2}{k_i^2}+\frac{1}{\alpha^2}\right]+\varepsilon_{MX}. \tag{28}$$

The integration over the angles gives the total cross section:

$$\sigma=\frac{2^{14}(2\alpha)^{1/2}(A_M+A_X)^3}{A_M(A_M+2A_X)^2}\frac{k_f}{k_i}\frac{\varepsilon_M^{5/2}\varepsilon_{MX}^{5/2}D_{X_2}^{3/2}-\varepsilon_a^{3/2}}{(\varepsilon_M^{1/2}+\varepsilon_a^{1/2}+2I_{X_2}^{1/2})^4}\frac{(1+\sqrt{I_{X_2}/\varepsilon_a})(1+2\sqrt{I_{X_2}/\varepsilon_a})\pi e^4}{(\varepsilon_M+D_{X_2}-\varepsilon_a)^2}$$
$$\times\left\{\frac{4}{B(C-A)^5}\left[\ln\left[\frac{C+B}{C-B}\right]-\ln\left[\frac{A+B}{A-B}\right]\right]+\frac{6}{(C-A)^4(C^2-B^2)}+\frac{2}{(C-A)^4(A^2-B^2)}\right.$$
$$\left.+\frac{4C}{(C-A)^3(C^2-B^2)^2}+\frac{6C^2+2B^2}{3(C-A)^2(C^2-B^2)^3}\right\}. \tag{29}$$

The differential and total cross sections are dependent on the c.m. energy, i.e., on the velocity. In actual experiments, the sources are such that there exists Maxwell-Boltzmann velocity distribution for the reacting as well as the produced atoms and molecules. It is, therefore, necessary to take the average of the cross sections over the relative velocity distribution. The velocity-averaged results for both differential and total cross sections as functions of temperature are found to be

$$\frac{d\overline{\sigma(T)}}{d\Omega}=\frac{\int_0^\infty\frac{d\sigma(v,T)}{d\Omega}e^{-\mu_iv^2/2kT}dv}{\int_0^\infty e^{-\mu_iv^2/2kT}dv} \tag{30}$$

and

$$\overline{\sigma(T)}=\frac{\int_0^\infty\sigma(v,T)e^{-\mu_iv^2/2kT}dv}{\int_0^\infty e^{-\mu_iv^2/2kT}dv}. \tag{31}$$

The observation of large cross sections of the production of alkali halide molecules in the collision between alkali-metal atoms and halogen molecules by Polanyi [1] has been followed by a number of experiments [24]. The most recent experiments have been performed by Davidovits and his collaborators [14,15].

We need values of electron affinities and dissociation energies in order to obtain explicit values of the cross section from our theory. For the halogen molecule, there exist two electron affinities: the vertical and the adiabatic [25–27]. If the electron transfer takes place during a time too short to permit adjustment in the internuclear distance of the molecule, the vertical electron affinity is the appropriate value, but if the internuclear distance adjusts adiabatically to the changing conditions in the region of the crossing point, the adiabatic electron affinity is to be used. The electron affinities that are accepted for calculations are given in Table I. The dissociation energies of the halogen molecular ions are given in Table II.

Taking the experimental values of dissociation energies of the halogen molecular ions and those of both the electron affinities of the halogen molecules, we have calculated $\bar{\sigma}(T)$ for the temperatures at which experiments have been performed [14,15]. The results obtained from our calculations along with σ_M and σ given by Eqs. (3) and (5), respectively, and those of experiment are given in Table III.

We find that the total cross sections obtained from our calculations are closer to the experimental results for chlorine if adiabatic electron affinity is used, and are

TABLE I. Electron affinities of Cl_2, Br_2 and I_2.

	Electron affinities in eV		
	Cl_2	Br_2	I_2
Vertical	1.3±0.4	1.2±0.5	1.7±0.5
Adiabatic	2.45±0.15	2.50±0.15	2.55±0.15

TABLE II. Dissociation energies of Cl_2^-, Br_2^-, and I_2^-.

Dissociation energy in eV		
Cl_2^-	Br_2^-	I_2^-
1.2±0.5	1.0±0.5	0.7±0.3

closer for bromine and iodine if vertical electron affinity is used. This might be due to the fact that both bromine and iodine are more reactive than chlorine to favor quick electron transfer. In addition to the harpoon mechanism, there are calculations for the total cross sections based on studies with translational capture [39] and potential-energy surfaces used in classical trajectory calculations [28,31–38,40–43]. Even if they provide results for total cross sections reasonably close to experimental values, there is a lack of a proper physical description of the reactions. Our calculation accounts for the appropriate physical quantities which are supposed to influence the total cross section.

Regarding the energy dependence of the total cross section, it is usually reported [15(a), 40, 44] that it is rather weak. However, a few experimental results [20,45] show strong energy dependence. On the basis of our calculations, the variations of cross sections with c.m. energy are given in Fig. 4. They show that for every reaction there exists a threshold energy given by

$$E_{\text{th}}=\varepsilon_M+D_{X_2}-\varepsilon_{MX} , \tag{32}$$

and the cross section attains the peak value very sharply and then falls off with increase in energy. For a given alkali-metal atom, the variation gets sharper with increasing order of peak value from Cl_2 to I_2. Again for a given halogen molecule, the variation is broader with increasing order of peak value from Na to Cs. We hope that improved experimental techniques may show a dependence of the total cross section on energy similar to that found in our results.

There are quite a number of both experimental and theoretical studies [16–20,46] for molecular-beam kinetics that investigate the angular distribution of the alkali halide produced in the reactive collision between an alkali-metal atom and a halogen molecule. Mostly the angular distribution is calculated for the relative intensity in arbitrary units for the c.m. system by fixed velocity approximation (FVA) at the most probable velocity making the transformation of the measured laboratory distribution. The results are found to show the following characteristics.

(a) The angular distribution of the alkali halide product is strongly forward peaked, the backward intensity being

TABLE III. Comparison, between experimental as well as other theoretical results with those of our calculations for production cross sections of MX in $M+X_2\rightarrow MX+X$.

M	X_2	ε_M (eV)	D_{X_2} (eV)	T (K)	ε_a (eV)	σ_M (Å^2)	σ (Å^2)	$\bar{\sigma}(T)$ (Å^2)	σ_{expt} (Å^2)
Na	Cl_2	5.14	2.48	1015	1.30	44.17	16.31	41.83	124±7.69
					2.45	90.02	24.37	74.79	
K	Cl_2	4.34	2.48	1015	1.30	70.49	21.38	65.75	154±6.16
					2.45	182.36	34.11	110.07	
Rb	Cl_2	4.18	2.48	1015	1.30	78.54	22.67	75.40	190±8.36
					2.45	217.66	36.75	177.94	
Cs	Cl_2	3.89	2.48	1015	1.30	97.11	25.34	90.71	196±6.66
					2.45	314.15	42.39	195.56	
Na	Br_2	5.14	1.97	973	1.20	41.96	18.65	114.51	116±5.80
					2.50	93.47	30.65	146.73	
K	Br_2	4.34	1.97	973	1.20	66.07	24.95	152.32	151±9.51
					2.50	192.41	44.88	203.90	
Rb	Br_2	4.18	1.97	973	1.20	73.35	26.59	191.27	197±9.26
					2.50	230.80	48.90	267.55	
Cs	Br_2	3.89	1.97	973	1.20	90.02	30.00	208.11	204±7.75
					2.50	337.16	57.70	348.66	
Na	I_2	5.14	1.54	860	1.70	55.05	26.27	107.03	97±2.33
					2.55	97.11	38.19	190.58	
K	I_2	4.34	1.54	860	1.70	93.47	37.28	152.18	127±3.00
					2.55	203.31	58.75	313.59	
Rb	I_2	4.18	1.54	860	1.70	105.92	40.31	188.23	167±4.00
					2.55	245.18	64.32	395.71	
Cs	I_2	3.89	1.54	860	1.70	135.82	46.82	258.62	195±6.04
					2.55	362.79	78.54	417.68	

about 20% of the forward intensity.

(b) The shape of the angular distribution is strongly peaked forward for K, Rb, and Cs but less so for Na and very broad for Li.

(c) The steepness of the forward peak increases in the sequence of I_2, Br_2, and Cl_2.

It is argued [16] that the very plausible chemical basis is the "harpoon mechanism" that appears to be consistent with all the dynamical properties found in the beam experiments. Our calculation provides the

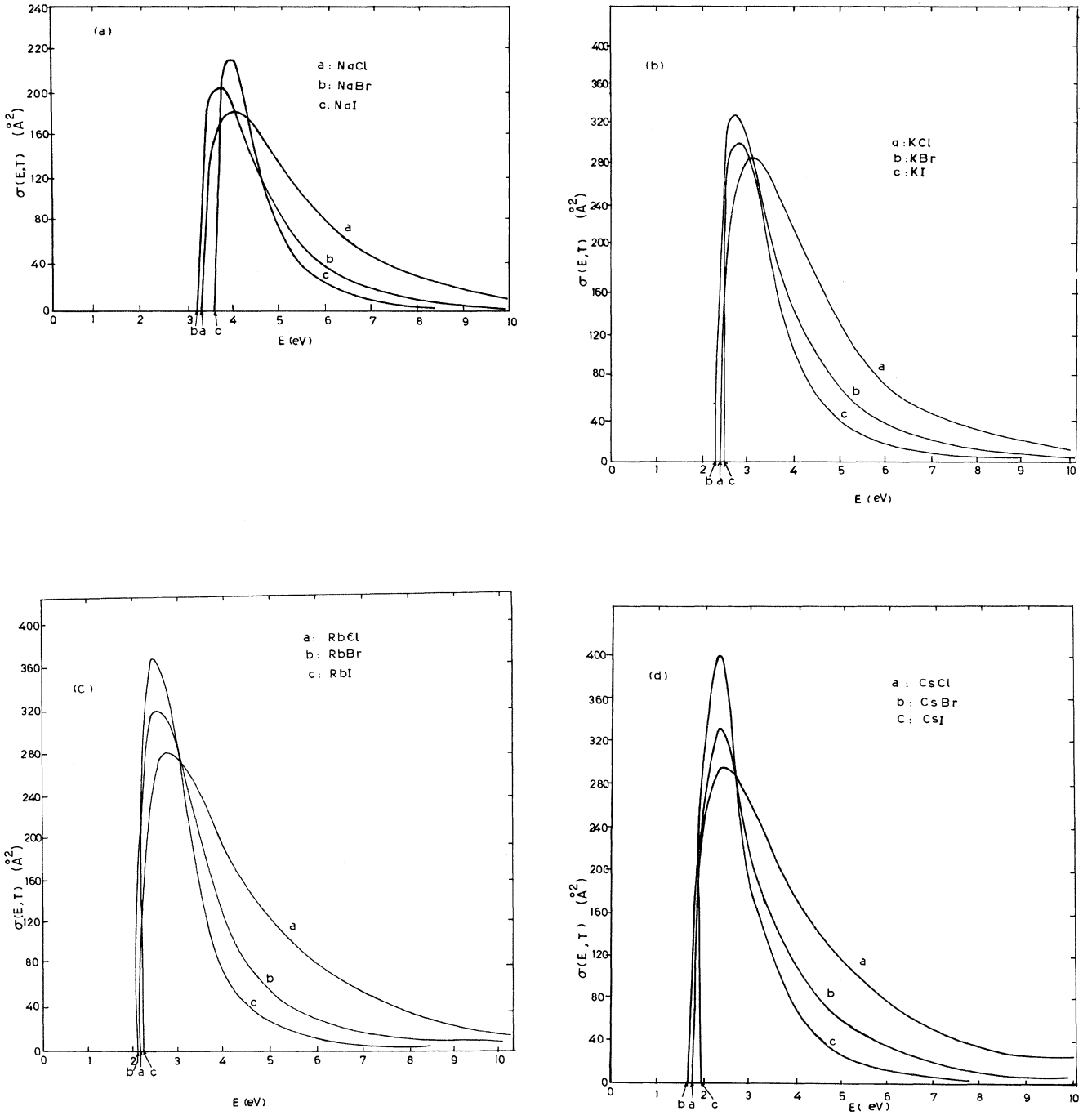

FIG. 4. Variation of the total cross section $\sigma(E,T)$ with the c.m. energy E.

velocity-averaged differential cross section, as given in Eq. (30).

The results obtained for the angular distribution of relative intensity in the c.m. frame on the basis of our calculation are given in Fig. 5. Our calculations are shown by solid curves, and experimental results by dark circles, as per Ref. [4] in Figs. 5(b) to 5(d), Ref. [16] in Figs. 5 (h) to 5(k), Ref. [18] in Fig. 5(f), and Ref. [19] in Figs. 5(a), 5(e),

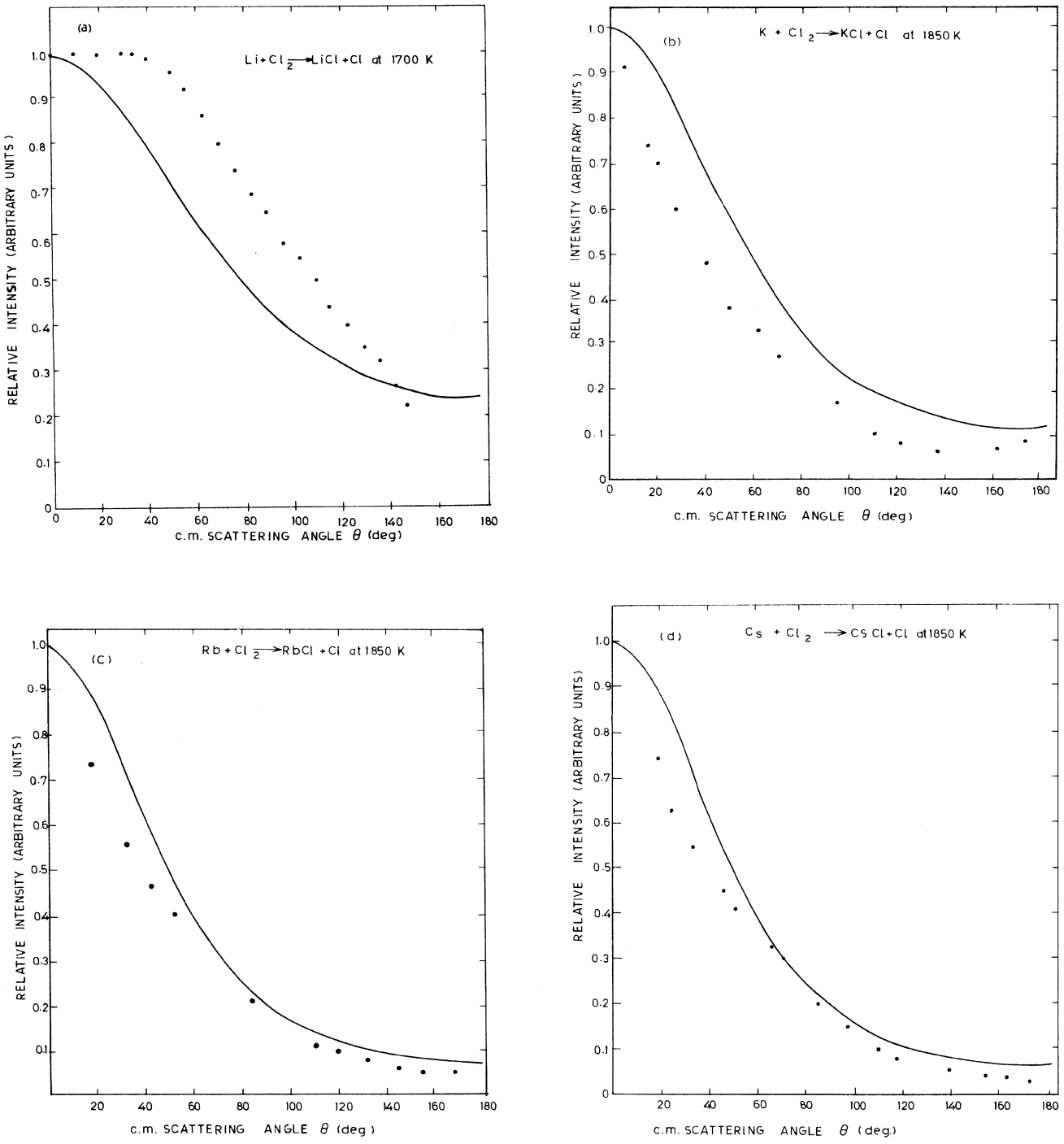

FIG. 5. Comparison, between experimental results and our calculations, for the variation of the relative c.m. angular distributions.

and 5(g). We observe that all the distributions of alkali halide products are forward peaked and are, for a given halogen molecule, in increasing order of steepness for alkali-metal atoms from Li to Cs. Even though it is suggested [12] that the c.m. angular distributions have practically no dependence on alkali-metal atoms for a given halogen molecule, our results show, in a unique manner, their variation quite clearly, in agreement with experimental results [16–19]. We hope that the variation of the distributions from atom to atom, particularly for K, Rb, and Cs was not clear due to inadequate experimental techniques. The experimental distributions for Li and Na

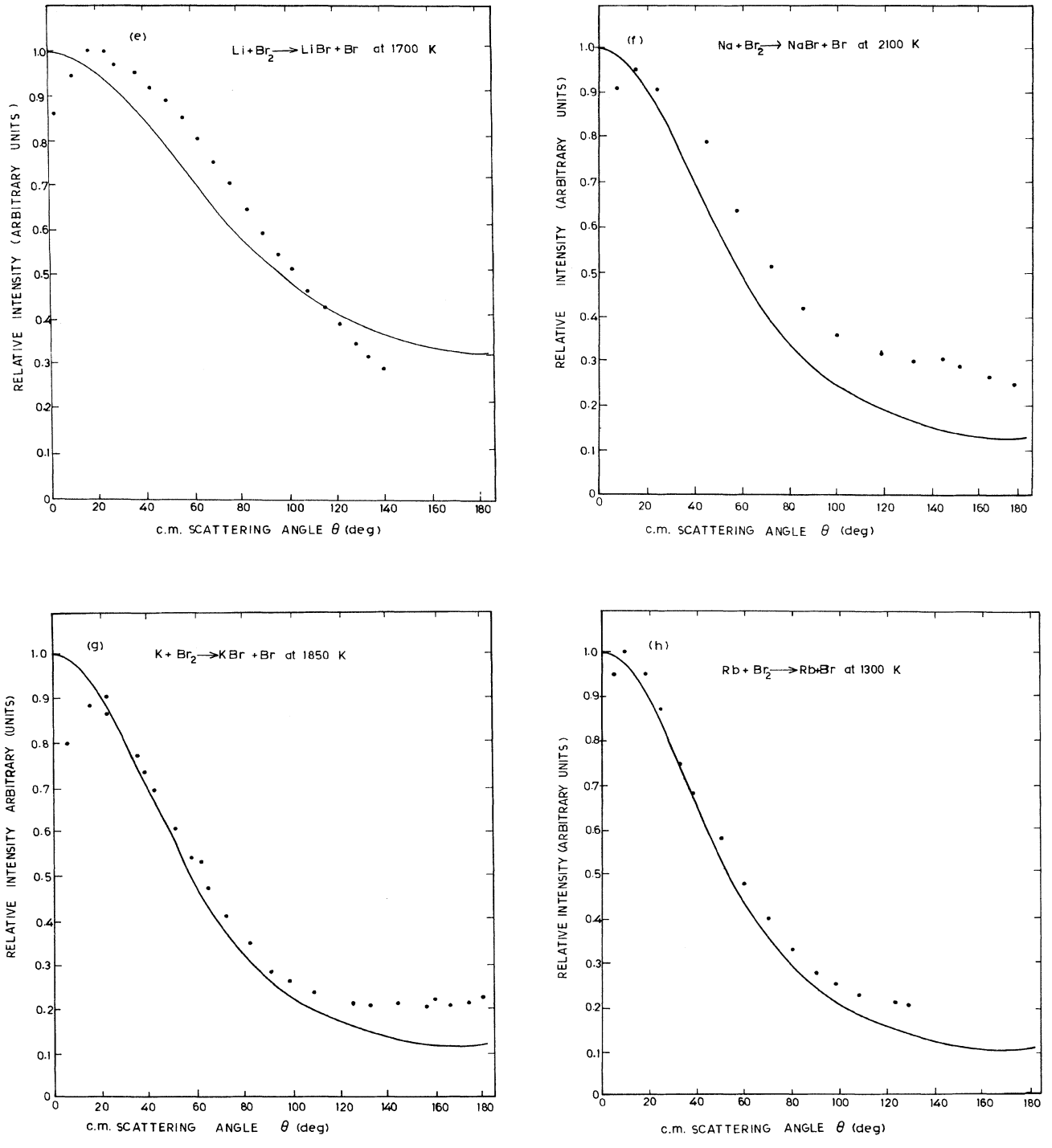

FIG. 5. (*Continued*).

are broader than those from our calculations. This might be due to the fact that a lighter alkali-metal ion reaches the halogen molecular ion in the early stage of its dissociation, compared to the heavier one, and thus dominates the reaction features. Our calculations reveal the increase in the steepness of the forward peak in the sequence of I_2, Br_2, and Cl_2, which is not in agreement with experimental results for the distribution for K and Cs with I_2. This might be due to the fact that K and Cs behave like light alkali-metal atoms compared to the iodine molecule. It is also found that the backward intensities ($\theta_{c.m.} > 90°$) are about 20% of the corresponding

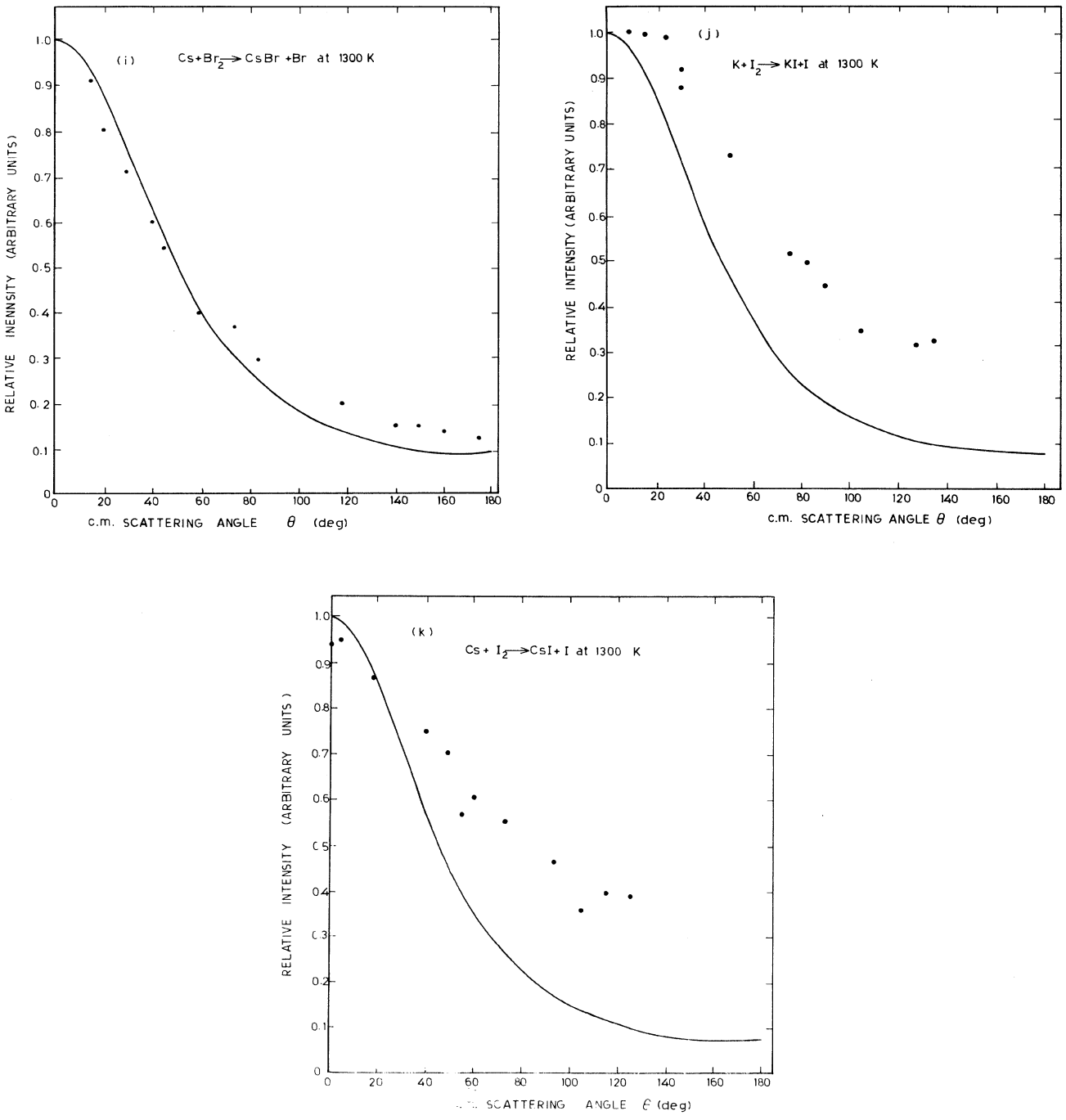

FIG. 5. (*Continued*).

forward intensities ($\theta_{c.m.} < 90°$) of the alkali halide products, except for LiCl and LiBr being 40% and 48%, respectively. The lightness of Li might be the explanation for this.

IV. DISCUSSION

We have used a Feynman-diagram approach to the harpoon mechanism for the reactive collisions between alkali-metal atoms and halogen molecules resulting in the formation of alkali halide molecules. We have obtained the variation of the cross section with c.m. energy, the velocity average of both differential and total cross sections, and their dependence on temperature. We hope that our method can be employed for many complex atomic and molecular collision processes.

ACKNOWLEDGMENTS

One of us (B.C.M.) acknowledges the use of the computer facility of the Institute of Physics, Bhubaneswar, and the help rendered by B. C. Parija and B. K. Panda in carrying out numerical calculations.

[1] M. Polanyi, *Atomic Reactions* (Williams and Norgate, London, 1932).
[2] M. G. Evans and M. Polanyi, Trans. Faraday Soc. **35**, 178 (1939).
[3] W. Ton *et al.*, J. Appl. Phys. **34**, 3635 (1963).
[4] S. Datz *et al.*, J. Chem. Phys. **41**, 1153 (1964); **44**, 1149 (1966); **47**, 993 (1967); **48**, 5352 (1968).
[5] D. R. Herschback, Adv. Chem. Phys. **10**, 319 (1966).
[6] J. L. Magee, J. Chem. Phys. **8**, 687 (1940); **61**, 562 (1957).
[7] M.A.D. Fluendy and K. P. Lawley, *Chemical Applications of Molecular Beam Scattering* (Chapman and Hall, London, 1973).
[8] R. K. Janev, Adv. At. Mol. Phys. **12**, 1 (1976).
[9] R. D. Cannon, *Electron Transfer Reactions* (Butterworths, London, 1980).
[10] M. S. Child, Mol. Phys. **16**, 313 (1969).
[11] R. Grice, Ph.D. thesis, Harvard University, Cambridge, MA, 1968.
[12] R. W. Anderson, Ph.D. thesis, Harvard University, Cambridge, MA, 1968.
[13] T. T. Warnock *et al.*, J. Chem. Phys. **46**, 1685 (1967).
[14] S. A. Edelstein and P. Davidovits, J. Chem. Phys. **55**, 5164 (1971).
[15] (a) J. Maya and P. Davidovits, J. Chem. Phys. **59**, 3143 (1973); (b) **61**, 1082 (1974).
[16] J. H. Birely *et al.*, J. Chem. Phys. **47**, 993 (1967).
[17] R. Grice and P. B. Empedocles, J. Chem. Phys. **48**, 5352 (1968).
[18] J. H. Birely *et al.*, J. Chem. Phys. **51**, 5461 (1969).
[19] D. D. Parrish and R. R. Herm, J. Chem. Phys. **49**, 5544 (1968); **51**, 5467 (1969).
[20] K. T. Gillen *et al.*, J. Chem. Phys. **54**, 2831 (1971).
[21] T. Pradhan and A. Khare, Pramana **6**, 312 (1976).
[22] B. C. Mishra and T. Pradhan, Pramana **15**, 291 (1980).
[23] T. Tietz, Phys. Rev. **124**, 493 (1961); Nuovo Cimento **62B**, 309 (1969).
[24] There is quite a large number of experiments that have been performed by different groups with repetitions after subsequent improvements in experimental conditions. The up-to-date experiments that can be considered for discussion are stated in Refs. 14 and 15.
[25] R. E. Minturn, S. Datz, and R. L. Becker, J. Chem. Phys. **44**, 1149 (1966).
[26] R. Grice, Adv. Chem. Phys. **30**, 247 (1975).
[27] *Alkali Halide Vapours,* edited by P. Davidovits and D. L. McFadden (Academic, New York, 1979).
[28] E. M. Goldfield *et al.*, J. Chem. Phys. **82**, 3179 (1985).
[29] E. M. Goldfield *et al.*, J. Chem. Phys. **82**, 3191 (1985).
[30] A. W. Kleyn *et al.*, Phys. Rep. **90**, 1 (1982).
[31] E. A. Gislason and J. G. Sachs, J. Chem. Phys. **62**, 2678 (1975).
[32] N. C. Blais, J. Chem. Phys. **49**, 9 (1968).
[33] M. Godfrey and M. Karplus, J. Chem. Phys. **49**, 3602 (1968).
[34] P. J. Kuntz *et al.*, J. Chem. Phys. **50**, 4607 (1969).
[35] C. Nyeland and J. Ross, J. Chem. Phys. **54**, 1665 (1971).
[36] R. Duren, J. Phys. B **6**, 1801 (1973).
[37] M. A. D. Fluendy *et al.*, Chem. Phys. **13**, 425 (1976).
[38] T. B. Borne and D. L. Bemker, J. Chem. Phys. **69**, 1792 (1978); **69**, 1794 (1978).
[39] Same as Ref. [15], and references therein.
[40] R. W. Anderson and D. R. Herschbach, J. Chem. Phys. **62**, 2666 (1975).
[41] J. R. Stine and J. T. Muckerman, J. Chem. Phys. **65**, 3975 (1976).
[42] J. F. Cuderman, Phys. Rev. A **5**, 1687 (1972).
[43] A. Macias and A. Riera, Phys. Rep. **90**, 299 (1982).
[44] C. W. A. Evers, Chem. Phys. **30**, 27 (1978).
[45] A. Van der Meulen *et al.*, Chem. Phys. **7**, 1 (1975).
[46] G. H. Kwei and D. R. Herschbach, J. Chem. Phys. **51**, 1742 (1969).